

08

Role of the shadowing effect in the growth kinetics of III–V nanowires by molecular beam epitaxy

© V.G. Dubrovskii¹, M.V. Rylkova¹, A.S. Sokolovskii¹, Zh.V. Sokolova^{1,2}, S.V. Mikushev¹

¹ St. Petersburg State University, St. Petersburg, Russia

² St. Petersburg State University of Economics, St. Petersburg, Russia

E-mail: dubrovskii@mail.ioffe.ru

Received March 28, 2022

Revised April 8, 2022

Accepted April 11, 2022

A model for III–V nanowire (NW) growth in molecular beam epitaxy (MBE) is developed, which describes the NW growth by surface diffusion of adatoms influenced by the shadowing effect. It is shown that the shadowing effect strongly influences the growth kinetics in dense ensembles of NWs. A new solution for the NW length as a function of its radius and deposition thickness is obtained. A comparison is given for theoretical and experimental lengths of InP NWs grown on either adsorbing or reflecting substrates.

Keywords: nanowires, adatom diffusion, shadowing effect.

DOI: 10.21883/TPL.2022.06.53455.19202

Nanowires (NWs) of semiconductor compounds III–V (III–V NWs) are promising in view of creating new-generation nanoheterostructures for photonics and nanoelectronics, including those on silicon and other lattice-mismatched substrates [1–4]. Due to efficient relaxation of elastic stresses, the III–V NWs may be grown on silicon substrates without formation of mismatch dislocations [5,6], contrary to planar layers or nanoislands [7]. The III–V NWs are often synthesized by the method of molecular beam epitaxy (MBE) according to the vapor–liquid–crystal (VLC) mechanism when either Au [8] or Ga [9] is used as a catalyst. The MBE method allows growing III–V NWs without a catalyst according to the selective epitaxy (SE) mechanism [10]. The VLC and SE mechanisms are sometimes combined within one and the same sample depending on the NW radius and deposition conditions [11].

The MBE growth of the III–V NWs on unprocessed substrates where Au droplets are created by thermal annealing proceeds due to direct impingement of the semiconductor material into a droplet and to surface diffusion of the III–group adatoms [12–15]. In the case of MBE growth on processed substrates when the Au or Ga droplets are deposited in a regular array of the oxide mask openings, the III–V NW formation mechanism is temperature-dependent. At high temperatures, the most probable mechanism is reflection (reemission) of the III–group adatoms from the oxide mask surface [16–18]. At low temperatures, the mechanism of diffusion-controlled growth or a combination of two mechanisms is not excluded. In both cases, an important role is played by the shadowing effect [16,18,19] that consists in blocking a part of the substrate surface and lateral surface of the considered NW by adjacent NWs during MBE. In work [18], we have proposed an analytical model of the NW growth influenced

by the shadowing effect and reemission flux during MBE on reflecting substrates. The goal of this study was to construct a model of the NW diffusion-controlled growth influenced by the shadowing effect at all the growth stages, which distinguishes our approach from the earlier proposed models for growing solitary NWs [12–15].

The geometry we consider is illustrated in Fig. 1. All NWs have the same cylindrical shape R in radius and L in length. The size dispersion will be considered in a separate publication. Possible effects associated with secondary Ga droplet nucleation are neglected. The droplet contact angle at the NW vertex is β . The case of $\beta = 0$ corresponds to the absence of a droplet during SE. The NW surface density is $N = 1/(cP^2)$, where P is the pitch of regular array of openings in growing on the processed surface, c is the geometric factor. The NW growth is controlled by the III–group element flux $v = v_0 \cos \alpha$ [nm/s], where v_0 is the total flux, α is the beam angle with respect to the surface normal. The III–group atom desorption from all the surfaces is assumed to be absent. Effective deposition thickness $H = vt$ is proportional to the growth time t . Similarly to papers [12,13,15], we consider the case of NWs with constant radius $R = \text{const}$ and constant-volume droplets ($\beta = \text{const}$). Thus, the model is applicable to any III–V NWs with lengths shorter than the III–group adatom diffusion length on the lateral surface in the absence of radial growth [12,13,15,18].

Based on the material balance condition, we have

$$H = N\pi R^2 L + H_{2D}(1 - NS_c). \quad (1)$$

The first term is the NW volume per unity surface area, while the second one is the volume of a quasi-two-dimensional (2D) layer growing between NWs; the 2D layer mean thickness is H_{2D} . The S_c area free of the 2D layer is $S_c = \pi(R + \lambda_s)^2$, where λ_s is the surface

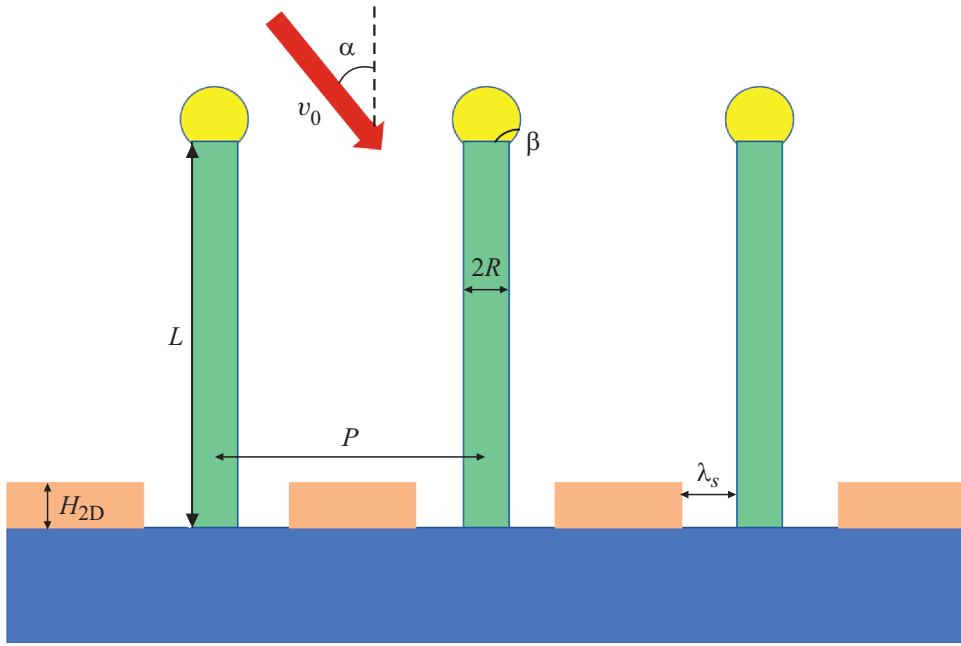


Figure 1. Illustration to the NW ensemble geometry.

diffusion length of the III–group adatom. Possibly, the growth of the 2D layer takes place also in the diffusion ring [14] when $S_c = \varphi\pi(R + \lambda_s)^2$, where φ is the fraction of adatoms coming from the diffusion ring to the NW vertex. Differentiating (1) with respect to time, obtain

$$v = N\pi R^2 \frac{dL}{dt} + v_{2D}(1 - NS_c), \quad (2)$$

where v_{2D} is the 2D layer growth rate. If the diffusion collection takes place from the entire substrate surface ($S_c = 1/N$), the rate of the NW vertical growth and NW length relevant to it are maximal and equal to [16,18]:

$$\left(\frac{dL}{dH}\right)_{\max} = \frac{1}{N\pi R^2} = \frac{cP^2}{\pi R^2},$$

$$L_{\max} = \frac{H}{N\pi R^2} = \frac{cP^2 H}{\pi R^2}. \quad (3)$$

In a more realistic case, when the diffusion collection occurs only from a part of the substrate surface, the following NW growth stages may be distinguished.

Stage 1 corresponds to $v = v_{2D}$ when shadowing does not affect the 2D layer growth. In this case, we obtain based on (2) that $dL/dH = S_c/(\pi R^2)$ and

$$L = \varphi \left(1 + \frac{2\lambda_s}{R} + \frac{\lambda_s^2}{R^2}\right) H. \quad (4)$$

This growth stage lasts as long as the growth rate $dL/dH = S_c/(\pi R^2)$ is higher than the rate of growth due to direct impingement into the droplet and adatom diffusion from the NW lateral surface (see relation (6) given below).

This corresponds to the NW length shorter than the first critical length L_1 :

$$L < L_1 = \frac{\varphi\pi \cotan \alpha (R + \lambda_s)^2}{2\xi} - \frac{\chi\pi R}{2\xi \sin \alpha}. \quad (5)$$

Stage 2 of the NW growth may be described by an equation conventionally used in modeling the kinetics of solitary NW formation [12–15]

$$\frac{dL}{dH} = \frac{2\xi \tan \alpha}{\pi R} L + \frac{\chi}{\cos \alpha}, \quad L(H = H_1) = L_1. \quad (6)$$

Here ξ is the fraction of adatoms coming from the NW lateral surface to its vertex [14], χ is the geometric function depending on angles α and β [20]. Effective deposition thickness H_1 matches with the NW length L_1 . Solution of relation (6) provides the exponential law of NW elongation defined as follows [13–15]:

$$L = \left(L_1 + \frac{\chi\pi R}{2\xi \sin \alpha}\right) \exp\left[\frac{2\xi \tan \alpha}{\pi R}(H - H_1)\right] - \frac{\chi\pi R}{2\xi \sin \alpha}. \quad (7)$$

Stage 2 lasts as long as $v_{2D} > 0$. Termination of the 2D layer growth means total blockage of the towards–surface flux by growing NWs due to the shadowing effect. From this, obtain the second critical shadowing length L_* and the Stage 2 range of NW lengths

$$L_1 \leq L \leq L_*, \quad L_* = \frac{\cotan \alpha}{2\xi NR} - \frac{\chi\pi R}{2\xi \sin \alpha}. \quad (8)$$

Notice that the L_* value (at $\xi = 1$) coincides with that found in [18].

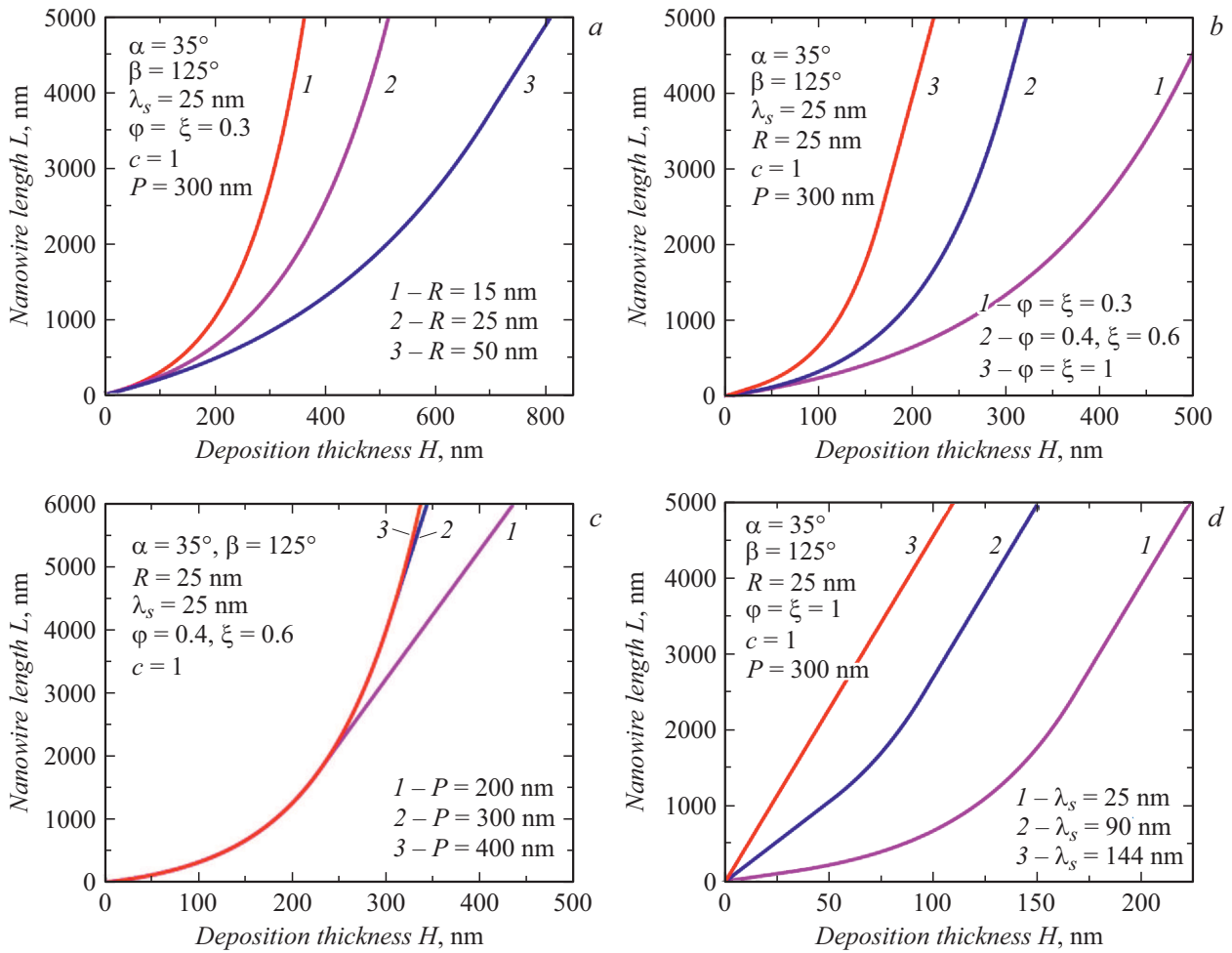


Figure 2. Dependences of the NW length L on the effective deposition thickness H , calculated via relations (4)–(9) at fixed $\alpha = 35^\circ$, $\beta = 125^\circ$, $\lambda_s = 25$ nm, $\varphi = \xi = 0.3$, $c = 1$, $P = 300$ nm at three different NW radii R (a); at fixed $R = 25$ nm and different combinations of parameters φ and ξ (b); at fixed $R = 25$ nm and three different values of P (c); at fixed $R = 25$ nm, $P = 300$ nm and three different diffusion lengths λ_s (d). The maximal diffusion length 144 nm corresponds to the diffusion collection of material from the entire surface and substrate, maximal NW length, and linear–in–time law of its elongation.

Stage 3 corresponds to the NW growth with the maximal rate (3) beginning from length L_* and effective deposition thickness H_* :

$$L = L_* + \frac{H - H_*}{N\pi R^2} = L_* + \frac{cP^2(H - H_*)}{\pi R^2}, \quad L > L_*. \quad (9)$$

This linear–in–time growth law is of the universal character and is valid for both the adsorbing and reflecting substrates because of the total blockage of the substrate surface and NW lower part [18].

Fig. 2 presents the L dependences on H calculated via relations (4)–(9) at fixed $\alpha = 35^\circ$, $\beta = 125^\circ$, $\lambda_s = 25$ nm, $\varphi = \xi = 0.3$, $c = 1$, $P = 300$ nm for three different NW radii: $R = 15, 25$ and 50 nm. Dependences $L(H)$ are two straight lines at small and large H interconnected by an exponential curve at intermediate H values. At the given H , the NW length increases with decreasing NW radius [12–15]. Fig. 2, b shows that the NW length increases with increasing φ and ξ . Fig. 2, c demonstrates the length

increase with increasing inter–NW distance P ; thereat, the exponential section of the $L(H)$ dependence increases at large P due to the increase in the shadowing length. Finally, Fig. 2, b shows that the NW length increases with increasing λ_s . The maximal value of λ_s corresponds to the material diffusion collection from the entire substrate surface and maximal NW length.

Fig. 3 presents experimental measurements of the length of the Au–catalytic InP NW with constant radius $R = 12$ nm versus H [17]. This NW was grown by the chemical beam epitaxy on the masked InP(111) B surface with a regular array of openings at $\alpha = 45^\circ$ and $cP^2 = 30\,625$ nm². Theoretical curves show that the reflecting surface model provides a better agreement with the experiment than the diffusion–controlled growth model. Hence, the first growth mechanism is more probable. The same conclusion was made in [16] for Ga–catalytic GaP NWs grown by MBE in regular arrays of openings in the SiO_x mask on Si(111). Along with this, the curves show

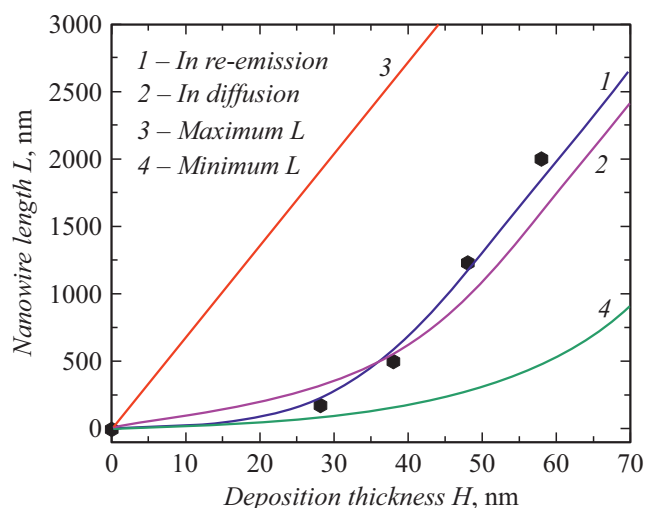


Figure 3. Experimental dependence of the length of the Au–catalytic InP NW with the constant radius of 12 nm obtained in [17] (symbols). Curve 1 represents the results of modeling the NW growth on a reflecting substrate [18], curve 2 was obtained based on relations (4)–(9) given in this paper at $\alpha = 45^\circ$, $\beta = 90^\circ$, $\varphi = \xi = 1$, $\lambda_s = 28$ nm and $cP^2 = 30\,625$ nm², curves 3 and 4 correspond to the maximal (at $S_c = 1/N$) and minimal (at $\lambda_s = 0$) rates of the diffusion-controlled growth on an adsorbing substrate.

that the NW length during the diffusion–controlled growth under the same conditions may be either larger or smaller (depending on the diffusion length λ_s) than in the case of the In flux reflection from the surface.

Thus, a model of the NW diffusion–controlled growth influenced by the shadowing effects was created for the first time, and new expressions were derived for the NW length as a function of the effective deposition thickness, inter–NW distance, and NW radii. The obtained results may be useful for describing and controlling the III–V NW morphology by, e. g., varying the inter–NW distances during their growth on masked surfaces.

Financial support

The study was supported by the Russian Scientific Foundation (project № 19-72-30004).

Conflict of interests

The authors declare that they have no conflict of interests.

References

- [1] Y. Zhang, A.V. Velichko, H. Aruni Fonseka, P. Parkinson, J.A. Gott, G. Davis, M. Aagesen, A.M. Sanchez, D. Mowbray, H. Liu, *Nano Lett.*, **21**, 5722 (2021). DOI: 10.1021/acs.nanolett.1c01461
- [2] V. Khayrudinov, M. Remennyi, V. Raj, P. Alekseev, B. Matveev, H. Lipsanen, T. Haggre, *ACS Nano*, **14**, 7484 (2020). DOI: 10.1021/acsnano.0c03184
- [3] L. Leandro, C.P. Gunnarsson, R. Reznik, K.D. Jöns, I. Shtrom, A. Khrebtov, T. Kasama, V. Zwiller, G. Cirlin, N. Akopian, *Nano Lett.*, **18**, 7217 (2018). DOI: 10.1021/acs.nanolett.8b03363
- [4] J. Sun, X. Zhuang, Y. Fan, S. Guo, Z. Cheng, D. Liu, Y. Yin, Y. Tian, Z. Pang, Z. Wei, X. Song, L. Liao, F. Chen, J.C. Ho, Z. Yang, *Small*, **17**, 2170190 (2021). DOI: 10.1002/sml.202170190
- [5] F. Glas, *Phys. Rev. B*, **74**, 121302(R) (2006). DOI: 10.1103/PhysRevB.74.121302
- [6] L.C. Chuang, M. Moewe, C. Chase, N.P. Kobayashi, C. Chang-Hasnain, *Appl. Phys. Lett.*, **90**, 043115 (2007). DOI: 10.1063/1.2436655
- [7] G.E. Cirlin, V.G. Dubrovskii, V.N. Petrov, N.K. Polyakov, N.P. Korneeva, V.N. Demidov, A.O. Golubok, S.A. Masalov, D.V. Kurochkin, O.M. Gorbenko, N.I. Komyak, V.M. Ustinov, A.Yu. Egorov, A.R. Kovsh, M.V. Maximov, A.F. Tsatusul'nikov, B.V. Volovik, A.E. Zhukov, P.S. Kop'ev, Zh.I. Alferov, N.N. Ledentsov, M. Grundmann, D. Bimberg, *Semicond. Sci. Technol.*, **13**, 1262 (1998). DOI: 10.1088/0268-1242/13/11/005
- [8] V.G. Dubrovskii, I.P. Soshnikov, G.E. Cirlin, A.A. Tonkikh, Yu.B. Samsonenko, N.V. Sibirev, V.M. Ustinov, *Phys. Status Solidi B*, **241**, R30 (2004). DOI: 10.1002/pssb.200409042
- [9] C. Colombo, D. Spirkoska, M. Frimmer, G. Abstreiter, A. Fontcuberta i Morral, *Phys. Rev. B*, **77**, 155326 (2008). DOI: 10.1103/PhysRevB.77.155326
- [10] S. Hertenberger, D. Rudolph, M. Bichler, J.J. Finley, G. Abstreiter, G. Koblmüller, *J. Appl. Phys.*, **108**, 114316 (2010). DOI: 10.1063/1.3525610
- [11] Q. Gao, V.G. Dubrovskii, P. Caroff, J. Wong-Leung, L. Li, Y. Guo, L. Fu, H.H. Tan, C. Jagadish, *Nano Lett.*, **16**, 4361 (2016). DOI: 10.1021/acs.nanolett.6b01461
- [12] J. Johansson, M.H. Magnusson, *J. Cryst. Growth*, **525**, 125192 (2019). DOI: 10.1016/j.jcrysgro.2019.125192
- [13] V.G. Dubrovskii, Yu.Yu. Hervieu, *J. Cryst. Growth*, **401**, 431 (2014). DOI: 10.1016/j.jcrysgro.2014.01.015
- [14] M.C. Plante, R.R. LaPierre, *J. Appl. Phys.*, **105**, 114304 (2009). DOI: 10.1063/1.3131676
- [15] J.C. Harmand, F. Glas, G. Patriarche, *Phys. Rev. B*, **81**, 235436 (2010). DOI: 10.1103/PhysRevB.81.235436
- [16] F. Oehler, A. Cattoni, A. Scaccabarozzi, J. Patriarche, F. Glas, J.C. Harmand, *Nano Lett.*, **18**, 701 (2018). DOI: 10.1021/acs.nanolett.7b03695
- [17] D. Dalacu, A. Kam, D.G. Austing, X. Wu, J. Lapointe, G.C. Aers, P.J. Poole, *Nanotechnology*, **20**, 395602 (2009). DOI: 10.1088/0957-4484/20/39/395602
- [18] V.G. Dubrovskii, *Nanomaterials*, **12**, 253 (2022). DOI: 10.3390/nano12020253
- [19] N.V. Sibirev, M. Tchernycheva, M.A. Timofeeva, J.C. Harmand, G.E. Cirlin, V.G. Dubrovskii, *J. Appl. Phys.*, **111**, 104317 (2012). DOI: 10.1063/1.4718434
- [20] F. Glas, *Phys. Status Solidi B*, **247**, 254 (2010). DOI: 10.1002/pssb.200945456